significant structure near 520 km depth[9,10,42], although several older velocity models do contain discontinuities or kinks near this depth[5,13–17]. These models were based mainly on analyses of P and SH wave refraction data and P wave slowness data recorded at arrays. These types of analyses cannot distinguish between sharp velocity discontinuities and local regions of steep velocity gradients. The long-period data shown in this paper also cannot distinguish between a discontinuity or enhanced velocity gradient at 520 km. The amplitude of the apparent Pp520p and Ss520s phases discussed in this paper are consistent with an impedance contrast at 520 km of ~3%, occurring within a gradient region less than about 25 km thick. But there is also some evidence for a 520-km reflector from quarry blast explosions[11] and short-period precursors to the phase P'P' (ref. 12). If these observations do represent reflections of high-frequency energy off a 520-km discontinuity, then the discontinuity must be relatively sharp (less than ~4 km thick), just as other short-period P'P' precursors imply a locally sharp 670-km discontinuity[44,45].

It is tempting to explain the possible existence of a 520-km discontinuity as representing the phase change between β-olivine and spinel, which occurs at about the right depth[1,12]. Recent high-pressure laboratory results, however, suggest that the change in velocity associated with this phase change occurs gradually and is quite small[46]. Other suggestions for possible phase changes near 520 km have included enstatite → spinel + stishovite[12] and garnet → garnet + perovskite[1], with more recent laboratory results indicating many complicated phase changes in the pyroxene/garnet system[47]. In general, predicted upper-mantle phase changes are highly dependent on composition and temperature, so conclusively identifying a specific phase change may be difficult. □

Received 30 November 1989; accepted 26 January 1990.

1. Ringwood, A. E. *Composition and Petrology of the Earth's Mantle* (McGraw-Hill, New York, 1975).
2. Ito, E. & Takahashi, E. *J. geophys. Res.* **94,** 10637–10646 (1989).
3. Anderson, D. L. & Bass, J. D. *Nature* **320,** 321–328 (1986).
4. Lehmann, I. *Ann. Geophys.* **15,** 93–118 (1959).
5. Hales, A. L., Muirhead, K. J. & Rynn, J. M. W. *Tectonophysics* **63,** 309–348 (1980).
6. Drummond, B. J., Muirhead, K. J. & Hales, A. L. *Geophys. J. R. astr. Soc.* **70,** 67–77 (1982).
7. Anderson, D. L. *J. geophys. Res.* **84,** 7555–7560 (1979).
8. Leven, J. H., Jackson, I. & Ringwood, A. E. *Nature* **289,** 234–239 (1981).
9. Walck, M. C. *Geophys. J. R. astr. Soc.* **76,** 697–723 (1984).
10. Grand, S. P. & Helmberger, D. V. *Geophys. J. R. astr. Soc.* **76,** 399–438 (1984).
11. Hoffman, J. P., Berg, J. W. & Cook, K. L. *Bull. seismol. Soc. Am.* **51,** 17–27 (1961).
12. Whitcomb, J. H. & Anderson, D. L. *J. geophys. Res.* **75,** 5713–5728 (1970).
13. Helmberger, D. & Wiggins, R. A. *J. geophys. Res.* **76,** 3229–3245 (1971).
14. Wiggins, R. A. & Helmberger, D. V. *J. geophys. Res.* **78,** 1870–1880 (1973).
15. Helmberger, D. V. & Engen, G. R. *J. geophys. Res.* **79,** 4017–4028 (1974).
16. Simpson, D. W., Mereu, R. F. & King, D. W. *Bull. seismol. Soc. Am.* **64,** 1757–1788 (1974).
17. Fukao, Y. *Geophys. J. R. astr. Soc.* **50,** 621–642 (1977).
18. Byerly, P. *Bull. seismol. Soc. Am.* **16,** 209–265 (1926).
19. Jeffreys, S. H. *Mon. Not. R. astr. Soc. Geophys. Suppl.* **3,** 401–422 (1936).
20. Johnson, L. R. *J. geophys. Res.* **72,** 6309–6325 (1967).
21. Nguyen-Hai *Ann. Geophys.* **15,** 285–346 (1963).
22. Husebye, E. & Madariaga, R. *Bull. seismol. Soc. Am.* **60,** 939–952 (1970).
23. Davies, D., Kelly, E. J. & Filson, J. R. *Nature* **232,** 8–13 (1971).
24. Gutowski, R. R. & Kanesewich, E. R. *Geophys. J. R. astr. Soc.* **36,** 21–32 (1974).
25. Ward, S. N. *Bull. seismol. Soc. Am.* **68,** 133–153 (1978).
26. Revenaugh, J. & Jordan, T. H. *J. geophys. Res.* **94,** 5787–5813 (1989).
27. Engdahl, E. R. & Flinn, E. A. *Science* **163,** 177–179 (1969).
28. Bolt, B. A. *Geophys. J. R. astr. Soc.* **20,** 367–382 (1970).
29. Adams, R. D. *Bull. seismol. Soc. Am.* **61,** 1441–1451 (1971).
30. Husebye, E. S., Haddon, R. A. W. & King, D. W. *J. Geophys.* **43,** 535–543 (1977).
31. Nakanishi, I. *Geophys. J.* **93,** 335–346 (1988).
32. Davis, J. P., Kind, R. & Sacks, I. S. *Geophys. J.* **99,** 595–604 (1989).
33. Vinnik, L. P. *Phys. Earth planet. Inter.* **15,** 39–45 (1977).
34. Faber, S. & Müller, G. *Bull. seismol. Soc. Am.* **70,** 487–508 (1980).
35. Barley, B. J., Hudson, J. A. & Douglas, A. *Geophys. J. R. astr. Soc.* **69,** 159–172 (1982).
36. Bock, G. & Ha, J. *Geophys. J. R. astr. Soc.* **77,** 593–615 (1984).
37. Faber, S. & Müller, G. *J. Geophys.* **54,** 183–194 (1984).
38. Baumgardt, D. R. & Alexander, S. S. *Bull. seismol. Soc. Am.* **74,** 1683–1702 (1984).
39. Kind, R. & Vinnik, L. P. *J. Geophys.* **62,** 138–147 (1988).
40. Paulssen, H. *J. geophys. Res.* **93,** 10489–10500 (1988).
41. Bock, G. *J. Geophys.* **64,** 73–81 (1988).
42. Dziewonski, A. M. & Anderson, D. L. *Phys. Earth planet. Inter.* **25,** 297–356 (1981).
43. Choy, G. L. & Richards, P. G. *Bull. seismol. Soc. Am.* **65,** 55–70 (1975).
44. Richards, P. G. *J. Geophys.* **38,** 517–527 (1972).
45. Lees, A. C., Bukowinski, M. S. T. & Jeanloz, R. *J. geophys. Res.* **88,** 8145–8159 (1983).
46. Weidnor, D. J., Sawamoto, H., Sasaki, S. & Kumazawa, M. *J. geophys. Res.* **89,** 7852–7860 (1984).
47. Jeanloz, R. & Thompson, A. B. *Rev. Geophys. Space Phys.* **21,** 51–74 (1983).

ACKNOWLEDGEMENTS. I thank J. Garmany, G. Masters and G. Nolet for advice regarding this work. This research was partially supported by the NSF.

In vivo alteration of telomere sequences and senescence caused by mutated *Tetrahymena* telomerase RNAs

Guo-Liang Yu, John D. Bradley, Laura D. Attardi & Elizabeth H. Blackburn*

Department of Molecular and Cell Biology, University of California, Berkeley, California 94720, USA

Mutating the CAACCCCAA sequence in the RNA component of telomerase causes the synthesis *in vivo* of new telomere sequences corresponding to the mutated RNA sequence, demonstrating that the telomerase contains the template for telomere synthesis. These mutations also lead to nuclear and cell division defects, and senescence, establishing an essential role for telomerase *in vivo*.

TELOMERES, the ends of eukaryotic chromosomes, are essential for the stabilization of linear chromosomes and the completion of chromosomal DNA replication[1,2]. Telomeres from diverse eukaryotes, including protozoans, yeasts, plants and mammals, consist of simple tandemly repeated G+C-rich sequences, with the G-rich sequence at the 3′ end of each DNA strand of a chromosome[2–5]. For example, the telomeric sequence of the ciliated protozoan *Tetrahymena thermophila* consists of TTGGGG·AACCCC repeats[6].

The G-rich strand of telomeric DNA is synthesized *in vitro* by telomerase[7], a ribonucleoprotein enzyme with an essential RNA component[8,9]. The *Tetrahymena* telomerase synthesizes repeats of the telomeric DNA sequence 5′-TTGGGG-3′ without requiring an added exogenous template[7–9]. Analogous telomerase activities have been identified in the ciliates *Oxytricha nova*[10] and *Euplotes crassus*[11], and recently in human (HeLa) cells[12]; each synthesizes its species-specific repeats onto the 3′ end of a telomeric sequence using the G-rich sequence as a primer.

Telomerase activity, originally proposed on the basis of *in vivo* studies of heterologous telomeres in yeast, readily explains

* To whom correspondence should be addressed.

several aspects of telomere behaviour *in vivo*[13-19]. Telomeres with various sequences are recognized as such and function as telomeres when transformed into yeast[13,20-22]; yeast-specific repeats are invariably added to the distal end of the foreign telomeric sequence[13,20]. This behaviour parallels the recognition of different telomeric sequences as primers by telomerases *in vitro*[7-12]. In many species the number of telomeric repeats on the end of a particular chromosome is variable, resulting in length heterogeneity of telomeric restriction fragments and their appearance as diffuse bands on agarose electrophoresis gels. This length heterogeneity could be caused by a dynamic equilibrium between incomplete semiconservative chromosome replication and telomere synthesis by telomerase[2,16], but the role of telomerase in telomere maintenance *in vivo* has not been tested directly.

The telomerase RNA genes from *T. thermophila* and *E. crassus* have been identified, cloned and sequenced[9,23]. Strikingly, both of these RNAs include a sequence that could serve as a template for the synthesis of species-specific telomeric repeats. The integrity of this sequence—5′-CAACCCCAA-3′—in the *Tetrahymena* telomerase RNA is essential for telomerase activity[9]. Furthermore, the analogous sequence 5′-CAAAACCCCAAA-3′ in the *Euplotes* telomerase RNA has been identified as the template strand sequence for *in vitro* synthesis of the repeated *Euplotes* telomeric sequence, TTTTGGGG (ref. 23). Although these *in vitro* experiments implicate the telomere-complementary sequence in the RNA as the template for telomere synthesis *in vitro*, there has been no direct demonstration that they function as templates *in vivo*.

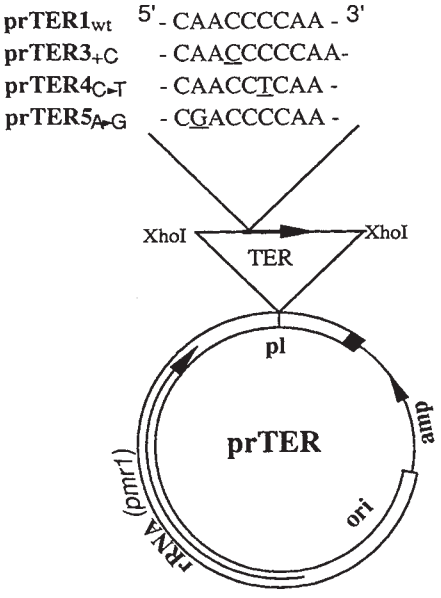

FIG. 1 Construction of prTER plasmids. The vector is shown as a circle. Thick open bar, rDNA sequences; thick solid bar, telomeric sequence; thin line, pBR322 sequences. The arrows show the transcription units of rRNA genes carrying the paromomycin resistance marker (*Pmr1*), ampicillin resistance gene (amp) and the telomerase RNA gene (TER). The TER genes were inserted in the polylinker (pl). The putative template sequences (+43 to +51 in the wild-type coding sequence)[9] are shown, with the mutated positions underlined. The telomerase RNA gene is transcribed in the same direction as the ribosomal RNA gene in these plasmids.

METHODS. A 550-bp *Hin*dIII–*Dde*I fragment containing the telomerase RNA gene was isolated from clone pCG1 (ref. 9). The fragment was blunt-ended, and *Xho*I linkers were ligated on both ends of the fragment. After digestion with *Xho*I, the fragment was inserted into the polylinker of prD4-1 to construct prTER1$_{wt}$. Site-directed mutagenesis was accomplished by a variation of the method of Kunkel[46]. A 1.6-kilobase (kb) *Hin*dIII fragment containing the TER gene and some of the flanking rDNA sequence from prTER1$_{wt}$ was inserted into the *Hin*dIII site of pUC119, and the plasmid was transformed into *Escherichia coli* strain RZ1032. Co-infection with bacteriophage M13KO7 resulted in the production of single-stranded uracil-containing plasmid. Oligonucleotides containing the desired mutations were annealed to the plasmid and used as primers for synthesis of the second strand. The DNA was transformed into *E. coli* strain DH5, and mutants were identified by sequencing single-stranded DNA obtained from individual transformants. In each of the three cases, ~50% of transformants carried the properly mutated plasmid. The 550-bp *Xho*I fragments containing the mutagenized TER genes were subcloned into the polylinker of the vector prD4-1.

We now present direct genetic evidence that the telomerase RNA contains the template for telomere synthesis *in vivo*. We altered the cloned *Tetrahymena* telomerase RNA gene in its putative template region by site-directed mutagenesis. Using a high-copy-number vector, we transformed *Tetrahymena* cells with three different mutant telomerase RNA genes. Two of these resulted in the *in vivo* synthesis of new telomeric sequences corresponding to the mutation in the template. In addition, telomeres in these transformants were longer than control cell telomeres. The third mutation led to telomere shortening. All three mutations, however, caused unexpected and striking phenotypic changes: specifically, nuclear and cell division were impaired, and viability was greatly decreased or the cells became senescent. These findings uncover an apparently new role for telomeres *in vivo* and indicate that the telomerase RNA gene is an essential gene.

Telomerase RNA overexpression

We subcloned the wild-type telomerase RNA gene (termed here the TER gene) from *T. thermophila*[9] into a circular ribosomal DNA plasmid vector, prD4-1. This vector, described in detail in ref. 24, carries the *cis*-acting replication control elements of the amplified rDNA and therefore replicates at high copy number ($>10^3$ copies per cell) in the macronucleus of *T. thermophila*. The polygenomic macronucleus, derived from the germ-line micronucleus, is the primary site of gene expression in ciliates. We inserted a 550-base pair (bp) *Hin*dIII–*Dde*I fragment containing the coding sequence for the 159-nucleotide *T. thermophila* telomerase RNA and its flanking regions[9] into the *Xho*I site in the polylinker in the plasmid vector to form plasmid prTER1$_{wt}$. This construct contains a ribosomal RNA gene carrying the dominant selectable paromomycin resistance marker (*Pmr1*) from the plasmid prD4-1 vector, and the wild-type telomerase RNA gene. The telomerase RNA transcription unit is in the same orientation as the ribosomal RNA gene (Fig. 1).

We transformed *T. thermophila* cells with circular plasmid prTER1$_{wt}$ by microinjection into the macronucleus as previously described[25,26]. Because the vector has a replication advantage over the recipient rDNA[24], the injected plasmid was maintained at high copy number. After growing the cells in nonselective medium for three days, we identified transformants by their ability to grow in selective medium containing 100 μg ml^{-1} paromomycin.

We obtained two prTER1$_{wt}$ transformants from 12 viable microinjected cells in one experiment, and three more independent transformants from pools of microinjected cells from another experiment. Southern-blot analysis showed that the telomerase RNA gene in these transformants, which is normally present as a single copy per haploid genome in the polygenomic macronucleus[9], was maintained on the amplified rDNA vector for more than 50 generations after microinjection (ref. 24, and data not shown).

To investigate the transcription of the introduced telomerase RNA gene, we isolated macronuclei from equal numbers of cells from a prTER1$_{wt}$ transformant line and from a control line transformed with the prD4-1 vector alone, and assayed them in nuclear run-off experiments. In prTER1$_{wt}$ transformants the telomerase RNA gene was transcribed at significantly higher levels than it was in the control prD4-1 transformant (Fig. 2*a*). To confirm that the increased rate of transcription reflected expression of the introduced telomerase RNA gene, we analysed

RNA from cells transformed with a vector carrying a mutant telomerase RNA gene, prTER3$_{+C}$ (described below). Because this mutant *TER* gene contains an additional C residue in the putative template region (see below, and Fig. 1), we expected its correct transcript to be one nucleotide longer than the wild-type transcript. Indeed, in primer extension experiments using total cellular RNA isolated from a prTER3$_{+C}$ transformant line, the main primer extension product was one nucleotide longer than that for the control RNA from the untransformed recipient cell strain (Fig. 2*b*). We confirmed this with an additional transformant line (data not shown). Therefore, the telomerase RNA in prTER3$_{+C}$ transformants contained the correct 5′ end, and most of the telomerase RNA in these cells was of the mutant type. Furthermore, the sensitivity of telomerase RNA gene transcription to α-amanitin in nuclear run-off experiments was similar to that of 5S RNA, rather than to that of rRNA (Fig. 2*c*), indicating that most of the labelled telomerase RNA in prTER1$_{wt}$ transformants was not a read-through product of RNA polymerase I transcription, but was expressed from its own promoter. Despite the increased rate of transcription resulting from its high gene dosage, northern-blot analysis showed that the accumulated level of telomerase RNA was the same in prTER1$_{wt}$ transformants as in control cells (Fig. 2*d*). Because telomerase is a complex of protein as well as RNA components[8,9], it is likely that the excess telomerase RNA in the transformants is degraded if it is unable to assemble into the telomerase ribonucleoprotein.

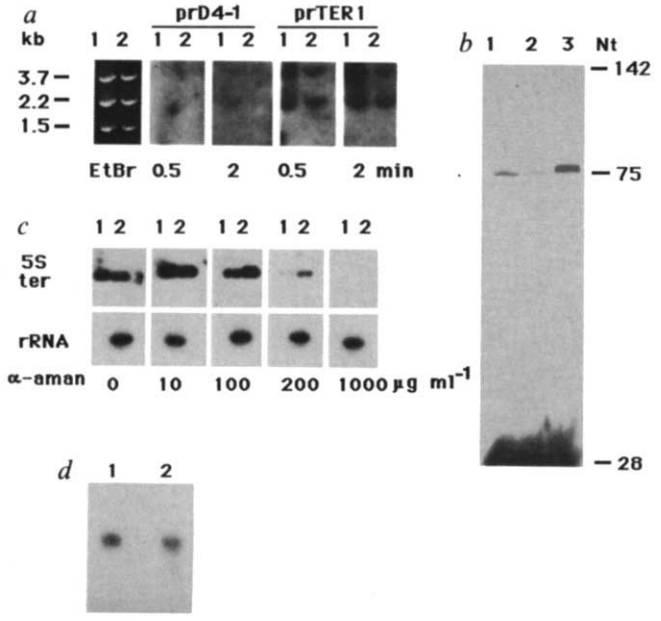

FIG. 2 Overexpression of the telomerase RNA gene. *a*, Nuclear run-off experiments. An equal number of nuclei isolated from prTER1$_{wt}$ and control prD4-1 transformant cells in late log phase ($\sim 2\times10^5$ cells ml^{-1}) were incubated with [α-^{32}P] rUTP and cold rATP, rCTP and rGTP in a buffer containing 0.1 M KCl, 20 mM HEPES–KOH buffer (pH 7.9), 5 mM dithiothreitol, 5% glycerol, 0.1 mM EDTA, 6 mM $MgCl_2$ (ref. 47) for 0.5 or 2 min at 30 °C. After treatment with protease K and phenol extraction, the radiolabelled RNA was used to probe Nytran filters carrying the immobilized cloned telomerase RNA gene. As shown in the ethidium bromide (EtBr)-stained photograph, each lane contains a mixture of a 3.7-kb uncut plasmid carrying the telomerase RNA gene and two restriction fragments (2.2 and 1.5 kb) resulting from digestion with *Bgl*II and *Xmn*I. *Bgl*II cuts at the beginning of the telomerase RNA coding region to generate the 2.2-kb fragment containing almost all the coding region, and the 1.5-kb fragment containing the upstream sequences. Lanes 1 and 2 contained 1 μg and 0.3 μg DNA, respectively. *b*, Primer extension of RNA from a prTER3$_{+C}$ transformant. Total RNA was isolated using guanidinium isothiocyanate[48]. To map the 5′ end of the telomerase RNA in prTER3$_{+C}$ transformants, a 28-nucleotide oligonucleotide complementary to the coding sequence (+47 to +64), downstream from the additional C, was labelled by polynucleotide kinase and extended using reverse transcriptase. Lane 1, recipient; lane 2, prTER3$_{+C}$ transformant from which the telomerase RNA gene had been lost (data not shown); lane 3, prTER3$_{+C}$ transformant containing the mutant telomerase RNA gene. Nt, nucleotides. *c*, Nuclear run-off assays in the presence of α-amanitin (α-aman). Assays were performed as described in *a*. Top panel, prTER1$_{wt}$ (lane 1) and *Tetrahymena* 5S DNA (lane 2); bottom panel, prD4-1 (rDNA probe). Concentrations of α-amanitin are shown at the bottom of the panel. *d*, Northern-blot analysis of TER RNA. Lane 1, recipient; lane 2, prTER1$_{wt}$ transformant. RNA was fractionated by agarose gel electrophoresis and the blot probed with nick-translated TER gene.

We found no significant difference in growth rates or morphology between cells of prTER1$_{wt}$ transformant lines and cells transformed with prD4-1 vector alone. In addition, telomere lengths in these prTER1$_{wt}$ transformants (examined in five independent prTER1$_{wt}$ transformant lines and in 14 single cell subclones from one of these lines) were the same as in untransformed controls (see below). Southern blotting showed that all these prTER1$_{wt}$ transformants had retained the introduced telomerase RNA gene at high copy numbers (data not shown). The absence of phenotypic changes in these wild-type gene transformants was consistent with the observed normal levels of accumulated telomerase RNA.

Altered telomere lengths

Using oligonucleotide-directed mutagenesis, we made three separate single nucleotide mutations in the telomere-complementary sequence of the telomerase RNA gene. These mutant plasmids were termed prTER3$_{+C}$, prTER4$_{C\to T}$ and prTER5$_{A\to G}$, the nucleotide alteration being indicated as a subscript (Fig. 1). We microinjected each mutant telomerase RNA gene in the rDNA vector into *Tetrahymena* macronuclei.

We analysed telomere length by Southern-blot analysis of *Bam*HI-digested DNA; as a probe we used [^{32}P] 5′ end-labelled telomeric $(T_2G_4)_2$ (top panel in Fig. 3), because we reasoned that the original telomeric sequence was likely to be still present in all telomeres, even if additional new telomeric sequences were synthesized. After *Bam*HI digestion, the high copy number rDNA telomeric fragment (shown in Fig. 3) was well separated from other macronuclear telomeric fragments, most of which migrated near limit mobility in agarose gel electrophoresis. The telomeric rDNA fragments in prTER3$_{+C}$ and prTER5$_{A\to G}$ transformants (lanes 3 and 5) had longer mean lengths and broader size distributions than did the telomeric fragments in control recipient cells and prTER1$_{wt}$ transformants (lanes 1 and 2). The telomeric fragments of other macronuclear chromosomes also appeared to be correspondingly longer and broader (data not shown). By contrast, in the prTER4$_{C\to T}$ transformant (lane 4) the rDNA telomeric fragment was significantly shorter than it was in the recipient strain and prTER1$_{wt}$ transformants.

The long telomere phenotype depended on the presence of the mutant telomerase RNA gene. We analysed telomere lengths in single cell subclones of a prTER3$_{+C}$ transformant by Southern blotting and probing with an rDNA fragment that hybridized to the telomeric fragment (Fig. 4). All of these subclones were derived from a single transformant clone that initially contained the mutant telomerase RNA gene at high copy number (data not shown) and long telomeres (Fig. 4*a*, lane 3). Of the 15 subclones that grew sufficiently for DNA analysis, seven still contained high, although variable, copy numbers of the mutant telomerase RNA gene on rDNA replicons; all of these seven contained long telomeres (Fig. 4*b*, lanes 1–3, 5, 11, 13 and 15). The remaining eight subclones had lost the mutant telomerase RNA gene through recombination of the rDNA vector with endogenous rDNA (refs 26, 27), and contained telomeres of normal length (Fig. 4*b*, lanes 4, 6–10, 12 and 14). That telomere length reverted to normal within 30 cell generations after the

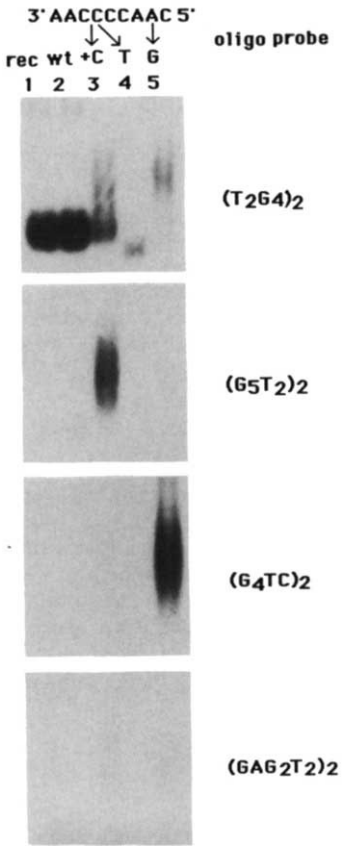

FIG. 3 Cells transformed by mutant telomerase RNA genes contain altered telomeric sequences. Genomic DNA from recipient (rec, lane 1), and cells transformed by prTER1$_{wt}$ (lane 2), prTER3$_{+C}$ (lane 3), prTER4$_{C\to T}$ (lane 4) and prTER5$_{A\to G}$ (lane 5), were digested with *Bam*HI and four identical sets of samples fractionated by agarose electrophoresis; blots were probed with oligonucleotides (oligo) shown on the right. wt, Wild type.

telomerase RNA gene was lost indicates that the presence of the mutant telomerase RNA is necessary for maintenance of long telomeres.

Novel telomere sequences

To analyse the telomeric sequences in the transformants, we probed identical blots containing equal aliquots of the set of transformant and control DNA samples with oligonucleotides with sequences corresponding to each mutation in the telomerase RNA gene (see Fig. 1): $(G_5T_2)_2$, $(GAG_2T_2)_2$ and $(G_4TC)_2$. Oligonucleotide $(G_5T_2)_2$ hybridized only to the telomeric fragments in the prTER3$_{+C}$ transformant (Fig. 3, lane 3). Conversely, the $(G_4TC)_2$ probe hybridized only with the telomeric fragment in the prTER5$_{A\to G}$ transformant (lane 5). By contrast, we could not detect any hybridization of the $(GAG_2T_2)_2$ probe that was specific to telomeric fragments in the prTER4$_{C\to T}$ transformant (lane 4), even though we used various hybridization and post-hybridization wash conditions and autoradiographic exposures. We conclude that in the prTER4$_{C\to T}$ transformant, unlike in the other two mutant telomerase RNA gene transformants, telomeres do not contain the altered telomeric sequence predicted from the mutation in the telomerase RNA.

To confirm that the mutated telomerase RNA gene dictates the synthesis of the predicted telomeric sequence *in vivo*, we cloned a telomeric fragment from a prTER5$_{A\to G}$ transformant. The insert in one clone that hybridized to $(G_4TC)_2$ was identified as an rDNA telomere by Southern blotting and DNA sequence analysis. The telomeric sequence of this clone is shown in Fig. 5. It includes several tandem repeats of the mutant telomeric sequence G_4TC located distally to a run of 30 G_4T_2 repeats. It is interesting that at two positions, a single wild-type repeat interrupts the total of 11 mutant repeat units, and an additional stretch of distal wild-type G_4T_2 repeats is also present.

The telomeric sequence is normally highly invariant in *Tetrahymena*; in previous studies, sequencing of > 2,400 nucleotides in 14 different telomere clones from wild-type *Tetrahymena* revealed only one different repeat—G_5T_2 (refs 28, 29). This contrasts with the variability that is characteristic of telomeric repeat sequences in some organisms (ref. 4; see ref. 3 for a review). We conclude that the mutant telomere containing G_4TC repeats was synthesized by copying the altered sequence in the mutated telomerase RNA.

Mutant phenotypes

Each of the three mutated telomerase RNA genes tested caused striking morphological changes and senescence when overexpressed in *Tetrahymena* cells. The prTER4$_{C\to T}$ transformants showed the most extreme senescence phenotype. We analysed three transformant lines, and isolated 48 and 24 single cells from two of them. None reverted and, after a week in culture, all 72 sublines were dead. Before they died, most prTER4$_{C\to T}$ transformant cells had rounded or irregular shapes, and were much larger than wild-type cells (Fig. 6, compare *a* and *c*). The macronuclei were also enlarged. The macronuclei were often highly irregular in shape and stained variably with (4′,6-diamidino-2-phenylindole (DAPI); Fig. 6*c*).

Using plasmid prTER3$_{+C}$, we obtained nine independent transformant lines. We also observed striking morphological and divisional changes in these lines. The prTER3$_{+C}$

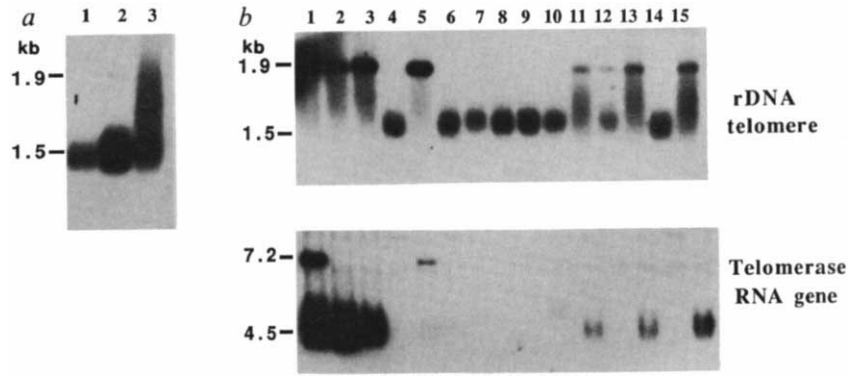

FIG. 4 Presence of a mutant telomerase RNA gene is required for long telomeres. *a*, Ribosomal DNA telomeres in recipient (lane 1), prTER1$_{wt}$ transformant (lane 2), and a prTER3$_{+C}$ transformant (lane 3). *b*, Southern blotting analysis of rDNA telomeres in single cell lines. Single cell lines from a prTER3$_{+C}$ transformant were isolated into 1 ml nonselective medium in multi-well tissue culture plates. Southern blots of DNA samples from 15 single cell lines were probed with rDNA or TER gene probes. Top panel, rDNA telomeres; bottom panel, TER gene. Previous work[24,26,27] showed that the rDNA vector recombines with the endogenous rDNA to form a linear molecule. The 7.2-kb fragment contains the TER gene in the circular form, whereas the 4.5-kb telomeric fragment contains the TER gene in the linear recombinant form.

transformant cells grew extremely large, with very irregular cell and nuclear shapes. Staining with DAPI (Fig. 6*b*) indicated that although macronuclear and cell divisions were greatly impaired, DNA replication was relatively unaffected. Multiple small nuclei, tentatively identified as micronuclei, were frequently visible (Fig. 6*b*). It is interesting that these phenotypic features are similar to those of the 'monster cells' generated at nonpermissive temperatures in temperature-sensitive cell division arrest (*cda*) mutants, isolated previously in *T. thermophila*[30,31]. The molecular basis of the *cda* mutants is not known.

To examine the senescence phenotypes of the prTER3$_{+C}$ transformants, we isolated, 3 days after the addition of paromomycin, each of 48 drug-resistant single cells from one transformant line into 1 ml nonselective medium. All subclones had monster phenotypes and grew very slowly, with 25 dying and only 23 growing sufficiently for DNA analysis. All 23 subclones had long telomeres (data not shown). From an 11-day-old stock culture of another transformant, we made 24 single-cell subclones. Nine subclones failed to divide further, whereas eight grew to saturation after one week, at which time most of the cells appeared normal. These eight saturated cultures were overgrown by cells that had lost the introduced telomerase RNA gene (see above and Fig. 4). But the remaining seven subclones grew only very slowly after one week, had monster phenotypes, and subsequently all single cells isolated from them failed to divide further—that is, they were senescent. These seven subclones had retained the mutant telomerase RNA gene and had long telomeres (see above and Fig. 4). We observed similar results to those seen with the prTER3$_{+C}$ transformant with the three prTER5$_{A\rightarrow G}$ transformant lines that we obtained; the 'monster' phenotype of these lines is shown in Fig. 6*d*.

In summary, all three alterations of the telomere-complementary sequence in the telomerase RNA caused impairment and eventual arrest of cell division in *Tetrahymena*; reversion of this phenotype occurred upon loss of the mutant telomerase RNA gene.

5' ···CTTTTACTCAATGTCAAAGAAATTATTAAATT(GGGGTT)$_{30}$

(GGGGTC)$_2$GGGGTT(GGGGTC)$_8$GGGGTTGGGGTC(GGGGTT)$_n$···3'

FIG. 5 Sequence of a novel telomere from transformed *Tetrahymena*. Total genomic DNA from a prTER5$_{A\rightarrow G}$ transformant was treated with T4 DNA polymerase in the presence of all four deoxynucleoside triphosphates (1 mM) to blunt the telomeric ends of the chromosomal DNA. The DNA sample was then digested with *Hin*dIII and ligated into the polylinker in plasmid pUC119 that had been linearized by digesting with *Hin*dIII and *Sma*I. The ligated DNA was transformed into *E. coli* and plated on LB plates containing 50 μg ml^{-1} ampicillin. Clones containing telomeric sequences were screened by colony hybridization, using labelled (G$_4$TC)$_2$ oligonucleotide as a probe. Southern analysis identified the cloned sequence as an rDNA telomere. The telomeric sequence of this clone is shown.

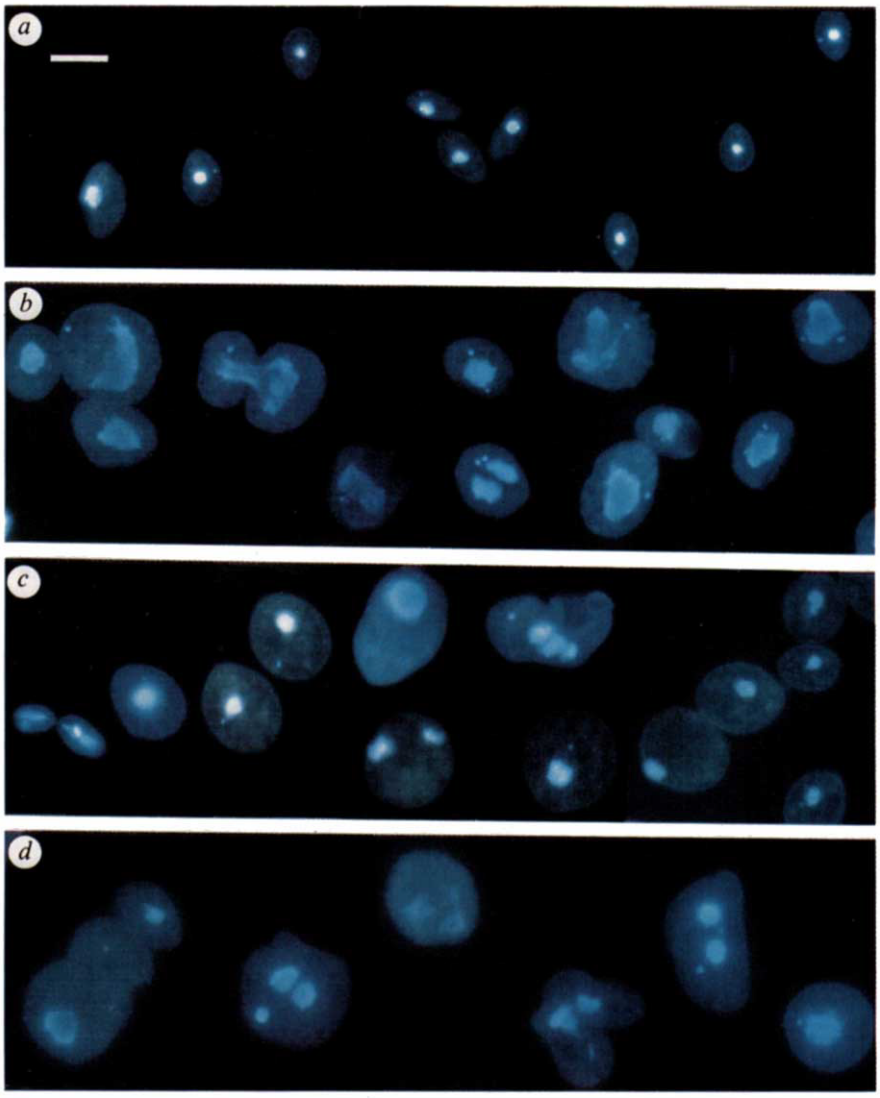

FIG. 6 *Tetrahymena* cells transformed with mutant telomerase RNA genes. Cells were fixed in 3.7% paraformaldehyde and stained with 0.1 μg ml^{-1} DAPI to visualize nuclei and show the shape of the cells, and photographed using a Zeiss Universal microscope. *a*, Wild-type cells; *b*, plasmid prTER3$_{+C}$ transformants; *c*, plasmid prTER4$_{C\rightarrow T}$ transformants; *d*, plasmid prTER5$_{A\rightarrow G}$ transformants. Bar, 50 μm.

Discussion

Telomerase RNA template. We changed the sequences of telomeres *in vivo* by transformation with two different mutated telomerase RNA genes containing an altered template sequence. Specifically, overexpression of the mutant telomerase RNA gene containing the sequence 5′-CGACCCCAA-3′ (mutated base underlined) in transformed cells resulted in incorporation of 5′-GGGGTC-3′ repeats. The presence of more-distal wild-type repeats in this mutant telomere suggests that although the mutant repeats were added onto the wild-type telomeric GGGGTT repeats, recombination between telomeres or growth after the mutant gene was lost from this cell had occurred. We similarly found that the mutated sequence 5′-CAACCCCCAA-3′ also specifies the synthesis of 5′-GGGGGTT-3′ repeats. These results establish that telomerase uses the telomeric sequence in the RNA as a template for telomere synthesis *in vivo*.

Telomere length regulation. The telomeres from the prTER3$_{+C}$ and prTER5$_{A\rightarrow G}$ transformants, which had altered telomere sequences, were longer than those in control cells. This indicates that the dynamic equilibrium between elongation and shortening of telomeres *in vivo* was shifted towards elongation. Although it is possible that these two changes in the telomerase template increase its activity *in vivo*, other data suggest that *in vivo*, a negative regulator of telomerase activity competes with telomerase for binding to the end of telomeres[32]. If changing the terminal sequences of a telomere reduces its binding affinity for the negative regulator, net telomerase activity could effectively increase. A candidate for such a negative regulator is a tightly binding sequence-specific telomere protein of the class that has been characterized in the ciliate *Oxytricha*[33–37]. The *Oxytricha* telomere protein has greater affinity for the *Oxytricha* telomeric sequence than for the *Tetrahymena* telomeric sequence[33]. When bound by these structural telomere proteins *in vitro*, chromosomal DNA ends are protected from exonuclease and methylation[33–37]. The rDNA telomeres in *Tetrahymena* are in a non-nucleosomal complex[38,39], which is likely to include analogous tightly bound proteins (E. H. Henderson, personal communication).

The prTER4$_{C\rightarrow T}$ transformants did not contain the altered telomeric sequence predicted from the change in the telomerase RNA template, and telomere length was decreased from ~300 to <200 bp of telomeric repeats compared with controls. Although other explanations are not ruled out, the results with prTER4$_{C\rightarrow T}$ transformants strongly indicate that the C→U change in the telomerase in these cells interferes with its activity, and that impairing the addition of telomeric repeats leads to telomere shortening and eventual loss, which would explain why the transformants become senescent. The inactivation could simply reflect inefficient use of dATP by the enzyme, because copying of the mutated template sequence would require incorporation of dATP by telomerase. Alternatively, the mutated C nucleotide could have some other function in the activity or formation of the telomerase complex. By overexpressing other mutated telomerase RNA genes we hope to test whether functions can be assigned to this nucleotide, as well as other specific nucleotides or regions in the telomerase RNA.

The telomerase RNA gene is the first non-ribosomal RNA gene to be used to transform *Tetrahymena* macronuclei. Although the endogenous wild-type gene was still present, the excess product from the introduced mutated gene produced a 'dominant' phenotype. The ability to overexpress genes in this ciliate system should be useful for other studies.

A novel function for telomeres. The telomere shortening and senescence phenotypes of the prTER4$_{C\rightarrow T}$ transformants strikingly parallel those of yeast cells that lack a functional *EST1* gene[17], and are consistent with the suggestion[17,40] that this gene encodes a component of telomerase. The unexpected observation that transformants with either lengthened or shortened telomeres had impaired cell division and senescence phenotypes now implicates telomeres in a previously unrecognized role. The increased length of the telomeres in prTER3$_{+C}$ and prTER5$_{A\rightarrow G}$ transformants was unlikely to have been deleterious, because wild-type telomeres of similar lengths are not associated with any growth or division abnormalities[15]. Likewise, the existence of certain heterologous telomeric sequences in yeast transformants is not associated with a discernible phenotype[13,20]. But when these heterologous telomeric sequences are maintained, the most distal sequences are invariably yeast-specific. By contrast, in the study described here, we expect that the novel telomeric sequence was added and present, at least initially, at the distal end of the normal repeat sequences. This indicates that the change in the distal telomeric sequence causes the observed deleterious effects in *Tetrahymena*.

That similar morphological and senescence phenotypes were observed with all three mutated genes suggests that they have a common basis. This is most likely to be an impaired interaction with a sequence-specific telomere binding protein analogous to that characterized in *Oxytricha*[33–37]. Our results indicate the involvement of such a sequence-specific telomeric DNA–protein interaction in cell or nuclear division. We propose that these protein–DNA interactions are either weakened in the transformants with altered telomere sequences, or eventually lost in the transformants with shortened telomeres, with similar consequences for both. In prTER4$_{C\rightarrow T}$ transformants, loss of cell viability from eventual macronuclear chromosome loss could be superimposed on this effect. This would explain the greater severity of the senescence phenotype in these cells.

How could telomeres be involved in nuclear and cell division? Telomeres are often found in the lamina under the nuclear envelope[41]. The telomeric DNA–protein complex of *Oxytricha* self-associates into very large polymeric forms[37], and *in vitro*, synthetic telomeric DNA sequences are bound by the intermediate filament proteins vimentin and nuclear lamins[42,43]. These observations indicate a possible association of telomeres with nuclear lamins. Second, macronuclear division in *Tetrahymena* and other ciliates does not involve nuclear envelope breakdown or visible centriolar organization of a mitotic spindle, and segregation of the acentric linear chromosomes that comprise the macronuclear genome depends on mechanisms not involving cetromeres. We note that in yeast, segregation of 2-micron circles and HM silencer-containing acentric plasmids requires, respectively, the proteins REP1 and SIR4 (ref. 44), which both share amino-acid sequence similarities to conserved domains in nuclear lamins[45]. Taken together, these observations suggest that telomeric interaction with nuclear lamin-like proteins could be involved in the acentric chromosome segregation and nuclear division of the macronucleus. Further analysis will be necessary to dissect the mechanism of this functional involvement of telomeric DNA structure in nuclear division and cell viability. □

Received 22 December 1989; accepted 23 January 1990.

1. Blackburn, E. H. *Cell* **37,** 7–8 (1984).
2. Blackburn, E. H. & Szostak, J. W. *A. Rev. Biochem.* **53,** 163–194 (1984).
3. Forney, J., Henderson, E. R. & Blackburn, E. H. *Nucleic Acids Res.* **15,** 9143–9152 (1987).
4. Richards, E. R. & Ausubel, F. M. *Cell* **53,** 127–136 (1988).
5. Moyzis, R. K. *et al. Proc. natn. Acad. Sci. U.S.A.* **85,** 6622–6626 (1988).
6. Blackburn, E. H. & Gall, J. G. *J. molec. Biol.* **120,** 33–53 (1978).
7. Greider, C. W. & Blackburn, E. H. *Cell* **43,** 405–413 (1985).
8. Greider, C. W. & Blackburn, E. H. *Cell* **51,** 887–898 (1987).
9. Greider, C. W. & Blackburn, E. H. *Nature* **337,** 331–337 (1989).
10. Zahler, A. M. & Prescott, D. M. *Nucleic Acids Res.* **16,** 6953–6972 (1988).
11. Shippen-Lentz, D. & Blackburn, E. H. *Molec. cell. Biol.* **9,** 2761–2764 (1989).
12. Morin, G. B. *Cell* **59,** 521–529 (1989).
13. Shampay, J., Szostak, J. W. & Blackburn, E. H. *Nature* **310,** 154–157 (1984).
14. Bernards, A., Michels, P. A. M., Lincke, C. R. & Borst, P. *Nature* **303,** 592–597 (1983).
15. Larson, D. D., Spangler, E. A. & Blackburn, E. H. *Cell* **50,** 477–483 (1987).
16. Shampay, J. & Blackburn, E. H. *Proc. natn. Acad. Sci. U.S.A.* **85,** 534–538 (1988).
17. Lundblad, V. & Szostak, J. W. *Cell* **57,** 633–643 (1989).
18. Sugewara, N. & Szostak, J. W. *Yeast* **2** Suppl. 373 (1986).
19. Perrot, M., Barreau, C. & Begueret, J. *Molec. cell. Biol.* **7,** 1725–1730 (1987).
20. Pluta, A. F. & Zakian, V. A. *Nature* **337,** 429–433 (1989).
21. Cross, S. H. *et al. Nature* **338,** 771–774 (1989).
22. Brown, W. R. A. *Nature* **338,** 774–776 (1989).
23. Shippen-Lentz, D. & Blackburn, E. H. *Science* **247,** 546–552 (1990).
24. Yu, G.-L. & Blackburn, E. H. *Proc. natn. Acad. Sci. U.S.A.* **86,** 8487–8491 (1989).

25. Tondravi, M. M. & Yao, M.-C. *Proc. natn. Acad. Sci. U.S.A.* **83,** 4369–4373 (1986).
26. Yu, G.-L., Hasson, M. & Blackburn, E. H. *Proc. natn. Acad. Sci. U.S.A.* **85,** 5151–5155 (1988).
27. Yu, G.-L. & Blackburn, E. H. *Molec. cell. Biol.* (in the press).
28. Budarf, M. L. & Blackburn, E. H. *Nucleic Acids Res.* **15,** 6273–6292 (1986).
29. Spangler, E. A., Ryan, T. & Blackburn, E. H. *Nucleic Acids Res.* **16,** 5569–5585 (1988).
30. Frankel, J., Nelsen, E. M., Jenkins, L. M. *Devl Biol.* **58,** 255–275 (1977).
31. Frankel, J., Jenkins, L. M. & DeBault, L. E. *J. Cell Biol.* **71,** 242–260 (1976).
32. Runge, K. W. & Zakian, V. A. *Molec. cell Biol.* **9,** 1488–1497 (1989).
33. Gottschling, D. E. & Zakian, V. A. *Cell* **47,** 195–205 (1986).
34. Price, C. M. & Cech, T. R. *Genes Dev.* **1,** 783–793 (1987).
35. Price, C. M. & Cech, T. R. *Biochemistry* **28,** 769–774 (1989).
36. Raghuraman, M. K., Dunn, C. J., Hicke, B. J. & Cech, T. R. *Nucleic Acids Res.* **17,** 4235–4253 (1989).
37. Raghuraman, M. K. & Cech, T. R. *Cell* **59,** 719–728 (1989).
38. Blackburn, E. H. & Chiou, S.-S. *Proc. natn. Acad. Sci. U.S.A.* **78,** 2263–2267 (1981).
39. Budarf, M. L. & Blackburn, E. H. *J. biol. Chem.* **261,** 363–369 (1986).
40. Lundblad, V. & Blackburn, E. H. *Cell* (in the press).
41. Agard, D. A. & Sedat, J. W. *Nature* **302,** 676–681 (1983).
42. Shoeman, R. L., Wadle, S., Scherbarth, A. & Traub, P. *J. biol. Chem.* **263,** 18744–18749 (1988).
43. Shoeman, R. L., Pfundstein, S., Scherbarth, A. J. & Traub, P. *J. biol. Chem.* (in the press).
44. Kimmerly, W. J. & Rine, J. *Molec. cell Biol.* **7,** 4225–4237 (1987).
45. Diffley, J. F. X. & Stillman, B. *Nature* **342,** 24 (1989).
46. Kunkel, T. A. *Proc. natn. Acad. Sci. U.S.A.* **82,** 488–492 (1985).
47. Labhart, P. & Reeder, R. H. *Cell* **45,** 431–443 (1986).
48. Kingston, R. E. in *Current Protocols in Molecular Biology* (eds Ausubel, F. M. *et al.*) (Wiley, New York, 1988).

ACKNOWLEDGEMENTS. We thank J. W. Sedat for help with photomicrography, and our colleagues in the laboratory for comments on the manuscript. We are grateful to Y.-S. Jin for assistance and technical expertise in photography. This work was supported by the NIH (E.H.B.) and the NSF (J.D.B.).

LETTERS TO NATURE

X-ray reflection from cold matter in the nuclei of active galaxies

K. A. Pounds*, K. Nandra*, G. C. Stewart*, I. M. George† & A. C. Fabian†

* X-ray Astronomy Group, Department of Physics and Astronomy, University of Leicester, Leicester LE1 7RH, UK
† Institute of Astronomy, University of Cambridge, Cambridge CB3 0HA, UK

THE evidence accumulated over the past few years for strong soft X-ray emission from active galactic nuclei[1–3] has been interpreted as black body emission from the innermost stable region of an accretion disk feeding the putative black hole at the centre of the active nucleus, a view given strong support by the rapid variability of some soft X-ray components[4]. More recently, new X-ray data from the Exosat and Ginga satellites have revealed a second indicator of optically thick matter in the vicinity of the active nucleus, in the form of an iron K-fluorescence line at ≈6.4 keV (refs 5–8). We report the discovery of two further common features of continuum absorption and reflection, revealed in a composite spectrum from twelve Ginga observations of Seyfert-type active galactic nuclei. Most of these spectral features are shown to be well modelled by reprocessing of the hard X-ray power-law continuum in a slab (or perhaps a disk) of cold matter. There is also evidence for a substantial line-of-sight column of photoionized material.

The fact that active galaxies radiate at least 10% of their bolometric luminosity in the hard X-ray band (~2–20 keV) was established over 10 years ago[9–11], and early spectral data showed this X-ray emission to be well described by a single power law, of energy index $a \approx 0.7$ (refs 12, 13). Later measurements modified this view, with the discovery by Exosat that many Seyfert-type, emission-line active galactic nuclei (AGNs) had excess soft X-rays below ~1 keV (refs 1, 3) and with Einstein Observatory data showing similar results for the higher-luminosity quasi-stellar objects[2]. The detection of rapid (of the order of hours) variability in the soft X-ray component, in several cases, supports its interpretation as thermal emission (~10^5 K) from optically thick matter close to the central power source[4]. It is then natural to associate this matter with the primary accretion process feeding the active nucleus; it could exist in an accretion disk or in clouds, sheets of filaments, the chief requirement being for the material to be sufficiently dense to survive the strong heating close to the central nucleus[14].

Further evidence for neutral matter in AGNs has recently been provided by the detection of an iron K-fluorescence line near 6.4 keV superimposed on the power-law continuum of several Seyfert-type AGNs[5–8]. A second, more controversial, finding in Ginga and also in some Exosat data, is an apparent steepening of the power-law slope with increasing X-ray flux[8,15]. Again, this is of particular interest in relation to theoretical predictions of slope changes arising from electron scattering effects in a highly compact source[16]. An alternative explanation of the same data has been proposed, however, in the form of a partially ionized, or 'warm', absorber along the line of sight to the X-ray nucleus[7,17]. Clarification of these more recent results has been hampered by the limited statistics of the available X-ray spectra, particularly above ~10 keV.

To attempt to redress this limitation, data from twelve Ginga observations of eight Seyfert-type AGNs have been superimposed, to produce a composite X-ray spectrum, Ginga-12. The objects chosen (Akn120, Mkn335, MCG-6-30-15, NGC3227, NGC4051, NGC5506, NGC5548 and NGC7314) are all bright in hard X-rays, individually having 'canonical' power-law slopes (from the same Ginga data) with an energy index ranging from $\alpha \approx 0.63$ to $\alpha \approx 0.85$ (with the exception of Mkn335 which had $\alpha \approx 1.1$). A simple power-law fit to the Ginga-12 data yielded a best-fitting energy index, $\alpha \approx 0.70$, in close agreement with the weighted mean slopes of the individual spectra, supporting the validity of the summing procedure. Of most interest are the data-minus-model residuals from this fit, shown in Fig. 1. In addition to the strong positive feature near 6 keV, there is a dip between ~8 and 12 keV and an excess above ~12 keV. Given that an iron K-fluorescence line is seen in each individual spectrum, together with some indications of K-edge absorption, it is natural to try a second spectral model, of a power law plus K-line and K-edge. The resultant fit has $\alpha \approx 0.64$ (with 90% confidence limits of 0.62–0.68), a small equivalent hydrogen absorbing column, $N_H \approx 4.1\ (3.0\text{–}5.3) \times 10^{21}$ cm^{-2}, plus a K-line and edge as detailed below. The fit is remarkably good for such a composite spectrum, with a reduced chi-squared (χ^2_r) of 1.5 (for 38 degrees of freedom), compared with 9.0 (for 41 degrees of freedom) for the single power-law fit. The residuals of the best-fitting power law (Fig. 1) may now be quantified.

The Fe K-line has a mean (rest-frame) energy of 6.28 (6.07–6.49) keV. Although not well constrained, the suggestion of a mean energy less than that of neutral iron (6.4 keV) is interesting, given the expectation of a significant gravitational redshift in the fluorescence from matter close to the central hole[18]. The mean equivalent width of the line, of ~110 (75–150) eV, is also consistent with that expected from fluorescence from optically thick matter subtending a large solid angle (for example, an accretion disk) to the hard X-ray source[19].

A large dip appears between ~8 and 12 keV. If this is due to Fe K-shell absorption, it corresponds to a large column density, of ~$1.2\ (0.7\text{–}1.9) \times 10^{23}$ H atoms cm^{-2} (assuming a solar abundance of iron), much greater than that implied by the small value of the Ginga-12 low-energy cutoff. One obvious explanation is that the line-of-sight material is strongly ionized, thereby having a reduced low-energy opacity. The best-fit edge energy, of ~7.9 (7.5–8.7) keV, supports this interpretation.

The third obvious feature in the residuals shown in Fig. 1 is an excess flux above ~12 keV, which can be modelled well between 10 and 35 keV by a flat power law, of energy index $\alpha \approx 0.45$. This is also seen in several of our individual spectra and provides the first clear evidence for a 'high-energy tail' in the continuum spectra of low-luminosity AGNs, consistent with